

Level Structure of N^{14}

J. K. BAIR, H. O. COHN, AND H. B. WILLARD
Oak Ridge National Laboratory, Oak Ridge, Tennessee

(Received April 25, 1960)

Yields and angular distributions of the gamma rays from the first and second levels in C^{13} following excitation by inelastic proton scattering have been measured. Levels are observed at bombarding proton energies 3.80 Mev ($\Gamma=100$ kev), 4.1 Mev ($\Gamma=150$ kev), 4.14 Mev, and 4.52 Mev ($\Gamma=150$ kev). The first three levels result in excitation of the first excited state and the last in excitation mainly of the second excited state of C^{13} . N^{14} excitation energies corresponding to these levels are 11.07 Mev, 11.3₅ Mev, 11.39 Mev, and 11.74 Mev. Possible spin and parity assignments are made on the basis of the γ -ray angular distribution of the 4.52-Mev level. The $C^{13}(p,n)N^{13}$ neutron yield has been rerun yielding better values of the resonant energies. Neutron angular distributions are given for several bombarding proton energies.

I. INTRODUCTION

THE level structure of the compound nucleus N^{14} between 11- and 12-Mev excitation energy has been previously investigated by means of C^{12} plus deuteron reactions and by the reaction $C^{13}(p,n)N^{13}$ with results summarized by Ajzenberg-Selove and Lauritsen.¹ Recently, Kashy, Perry, and Risser² have investigated the elastic scattering of protons from C^{13} . The present work reports an investigation of this region of excitation by measurements of the yield and angular distribution of the gamma rays from the 3.68- and 3.09-Mev levels in C^{13} following excitation by inelastic proton scattering. In addition, certain new measurements are presented on the $C^{13}(p,n)N^{13}$ reaction.

II. EXPERIMENTAL PROCEDURE

In general, target and bombarding techniques were essentially those described in the $C^{13}(p,n)N^{13}$ experiment previously published.³ However, the proton energy calibration had been revised⁴ since the neutron work so that energies given in the present paper are more reliable, especially at the higher values where saturation effects in the beam analyzing magnet previously caused some uncertainty. All data were taken with targets approximately 5 kev thick for 1.75-Mev protons.

Neutron yields were measured with a long counter and a suitably biased propane recoil counter. Since the energy threshold for inelastic excitation of even the lowest level in C^{13} is above the threshold for the (p,n) reaction, it is necessary to measure the gamma radiation in the presence of this neutron background. In this particular case the relative intensities were such that it was found possible to suitably reduce the neutron intensity by means of shielding without seriously effecting the spectrum of the (fortunately, relatively high energy) gamma rays as measured with a 3-in. diameter by 3-in.

high NaI(Tl) crystal. The shield used to take the data presented here consisted of 11 cm of lithiated paraffin, 3½ cm of Boral, 4½ cm of lithiated paraffin, and 0.6 cm of lead, in that order, with the lead nearest the detector.

III. GAMMA-RAY MEASUREMENTS

Figure 1 shows the gamma-ray pulse-height spectrum, at a proton bombarding energy of 4.75 Mev, as detected with the 3-in. by 3-in. NaI(Tl) crystal using the neutron shield described above. Peak V is the full energy peak for the 3.68-Mev radiation, peak IV consists of the full

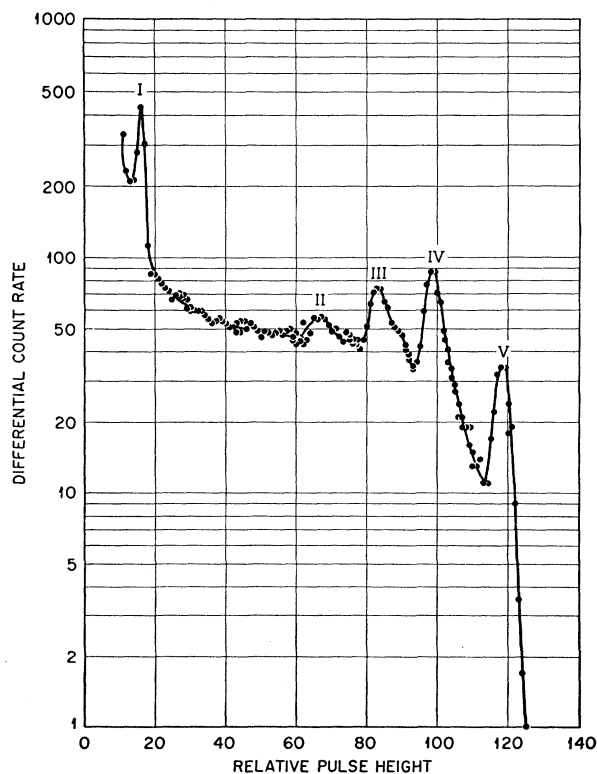


FIG. 1. $C^{13}(p,p'\gamma)C^{13}$ gamma-ray spectrum as seen by 3-in. \times 3-in. NaI(Tl) crystal through the neutron shield. The bombarding proton energy was 4.75 Mev. Peaks II through V are due to the 3.68-Mev and 3.09-Mev inelastic scattering gamma rays, peak I is due to annihilation radiation.

¹ F. Ajzenberg-Selove and T. Lauritsen, *Nuclear Phys.* **11**, 1 (1959).

² E. Kashy, R. R. Perry, and J. R. Risser, *Bull. Am. Phys. Soc.* **5**, 108 (1960).

³ J. K. Bair, J. D. Kington, and H. B. Willard, *Phys. Rev.* **90**, 575 (1953).

⁴ J. D. Kington, J. K. Bair, H. O. Cohn, and H. B. Willard, *Phys. Rev.* **99**, 1393 (1955).

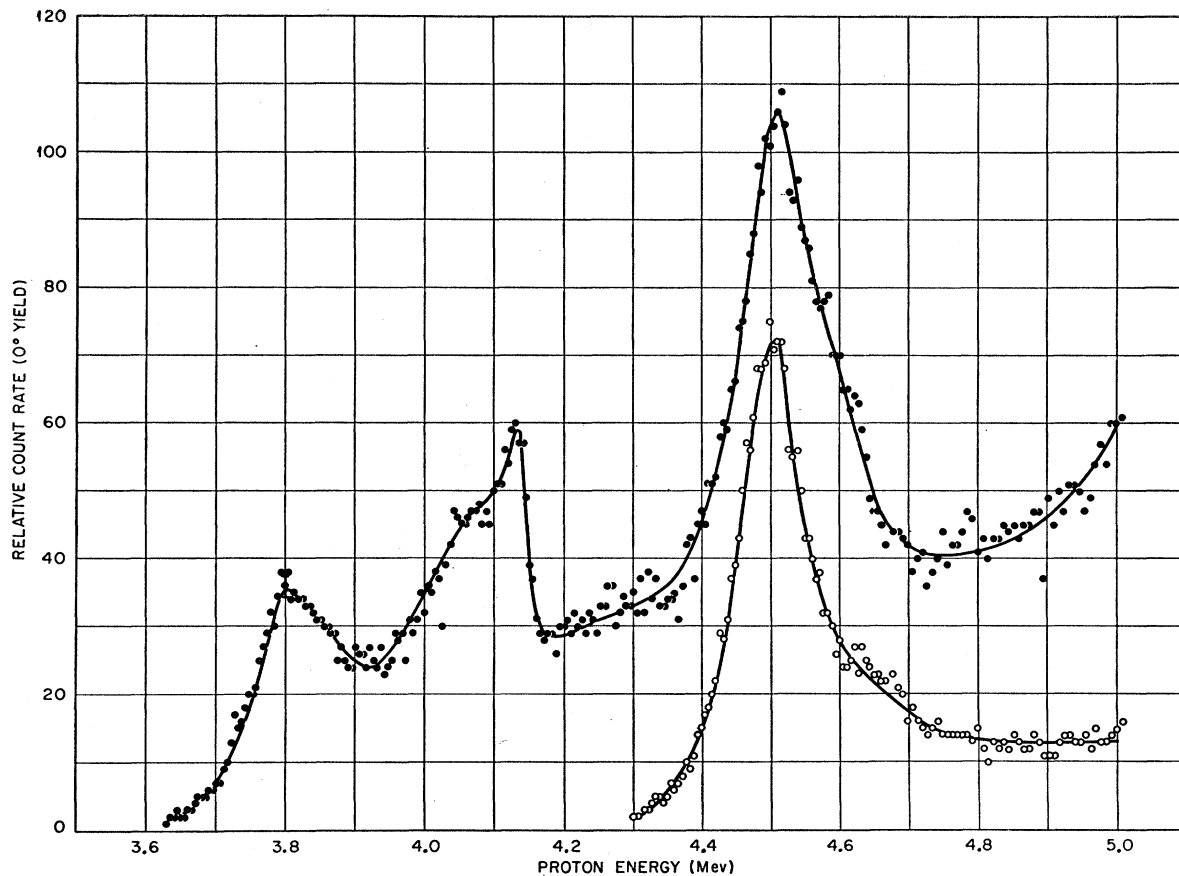


FIG. 2. $C^{13}(p, p'\gamma)C^{13}$ gamma-ray yield curve taken at 0° to the proton beam. The open points are for the 3.68-Mev gamma ray. Below about 4.3-Mev proton energy the solid points represent the yield of the 3.09-Mev gamma ray, above 4.3 Mev the solid points must be corrected for the presence of the higher energy gamma ray as described in the text.

energy 3.09-Mev radiation plus a contribution from the single escape peak of the 3.68-Mev gamma ray. Peak III consists of the two escape peak of the higher energy and the single escape peak of the lower energy gamma ray. Peak II is the two escape peak for the 3.09-Mev gamma ray. Peak I is due to annihilation radiation.

Figure 2 shows one set of yield curves obtained with the detector-neutron shield combination located at 0° with respect to the incoming proton beam and subtending a half angle of about $3\frac{1}{2}$ degrees. Similar curves at 90° to the proton beam, not shown, exhibit the same features. The data plotted are the readings of the highest channel in the full energy peaks. The open points represent the yield of the 3.68-Mev radiation. Below about 4.3-Mev proton energy, the high-energy gamma ray makes essentially no contribution to the 3.09-Mev gamma-ray data (solid points). Above 4.3 Mev the solid points must be corrected for the presence of the single escape peak of the 3.68-Mev radiation. By fitting a semiempirical curve of a "pure" 3.68-Mev gamma ray to the experimental spectrum, it can be shown that this correction to the yield can be made with reasonable accuracy by subtracting from the height of peak IV,

the height of peak V. Thus, above 4.3-Mev the true yield of the 3.09-Mev gamma ray can be represented by the difference between the solid and open points. It is evident that the maximum in the solid point curve at a proton energy of approximately 4.5 Mev is due almost entirely to the 3.68-Mev gamma ray and does not indicate a resonance in the 3.09-Mev gamma ray. There is, however, some indication of a broad maximum in the yield of the lower energy gamma ray at about 4.6-Mev bombarding energy. This maximum appears as a distortion on the high-energy side of the solid point curve, and is evident in both the 0° and 90° data. Columns 1, 2, 3, and 4 of Table I list the pertinent properties of the levels.

Angular distributions of the 3.09-Mev gamma ray were taken at twelve proton energies between 3.7 and 4.2-Mev, and of the 3.68-Mev gamma ray at 10 proton energies distributed over the 4.5-Mev resonance. The shield-detector combination subtended a half angle of $7\frac{1}{2}^\circ$ or less at the target for all the angular distribution measurements. All of the 3.09-Mev gamma-ray distributions were isotropic and are not shown. Figure 3 shows the distribution of the 3.68-Mev gamma ray at

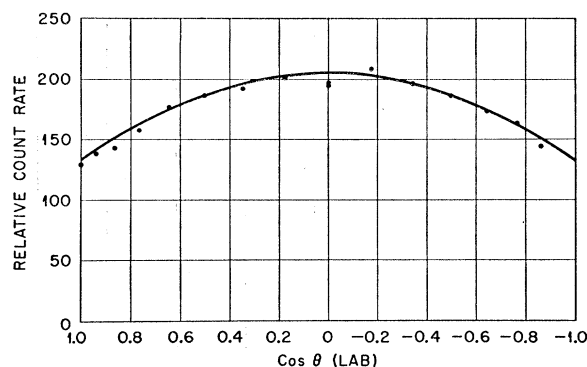


FIG. 3. The points are the experimental angular distribution of the 3.68-Mev inelastic gamma ray taken at the peak of the 4.5-Mev resonance. The solid curve is a plot of $1 - 0.35 \cos^2 \theta$.

the peak of the 4.5-Mev resonance. The data can be fitted with a $1 - 0.35 \cos^2 \theta$ distribution, which is shown as the solid curve.

IV. NEUTRON MEASUREMENTS

Since the published³ yield curve for the $C^{13}(p,n)N^{13}$ reaction has its energy scale based, in part, on the older, incorrect energy of the $F^{19}(p,\alpha\gamma)O^{16}$ resonances now known to be located at 1347 and 1374 keV, and also on analyzing magnet current, it was felt worthwhile to

TABLE I. Columns 1, 2, and 3 give the resonant proton energies for excitation of the 3.09-Mev inelastic scattering gamma ray, the 3.68-Mev inelastic scattering gamma ray, and an estimate of the experimental width, respectively. Column 4 gives the energy of excitation in the N^{14} compound nucleus. Column 5 gives the proton energy of the maximum in the forward neutron yield as measured in this experiment. Column 6 gives the difference between the value in Column 5 and that given in the older work of reference.^a Column 7 gives the proton energy of the maximum in the backward neutron yield, while Column 8 gives an estimate of the experimental width.

| | E_p Mev (3.09 γ) | E_p Mev (3.68 γ) | $W_{\frac{1}{2}}$ keV | E_x Mev | E_p Mev 0° neutrons | Δ keV | E_p Mev "180°" neutrons | $W_{\frac{1}{2}}$ keV |
|---|----------------------------------|----------------------------------|--------------------------|-------------------|--------------------------------|-----------------|------------------------------------|--------------------------|
| 1 | 3.80 | ... | 100 | 11.07 | 3.77 | 9 | 3.79 | 100 |
| 2 | ... | ... | ... | ... | 3.98 | 26 | 3.99 | 15 |
| 3 | 4.1 | ... | 150 | 11.3 ₅ | 4.1 | ... | 4.1 | 150 |
| 4 | 4.14 | ... | 30 | 11.39 | 4.15 | 31 | 4.13 | 30 |
| 5 | ... | 4.52 | 150 | 11.74 | 4.47 | 52 | 4.51 | 150 |

^a See reference 3

redetermine the energies of the maxima with the better techniques now available. In order to tie these measurements into the gamma-ray measurements, runs were made over the four most prominent maxima in the neutron yield curve measuring simultaneously the 90° gamma-ray yield, the 0° neutron yield as measured with a long counter, and the 170° neutron yield as measured

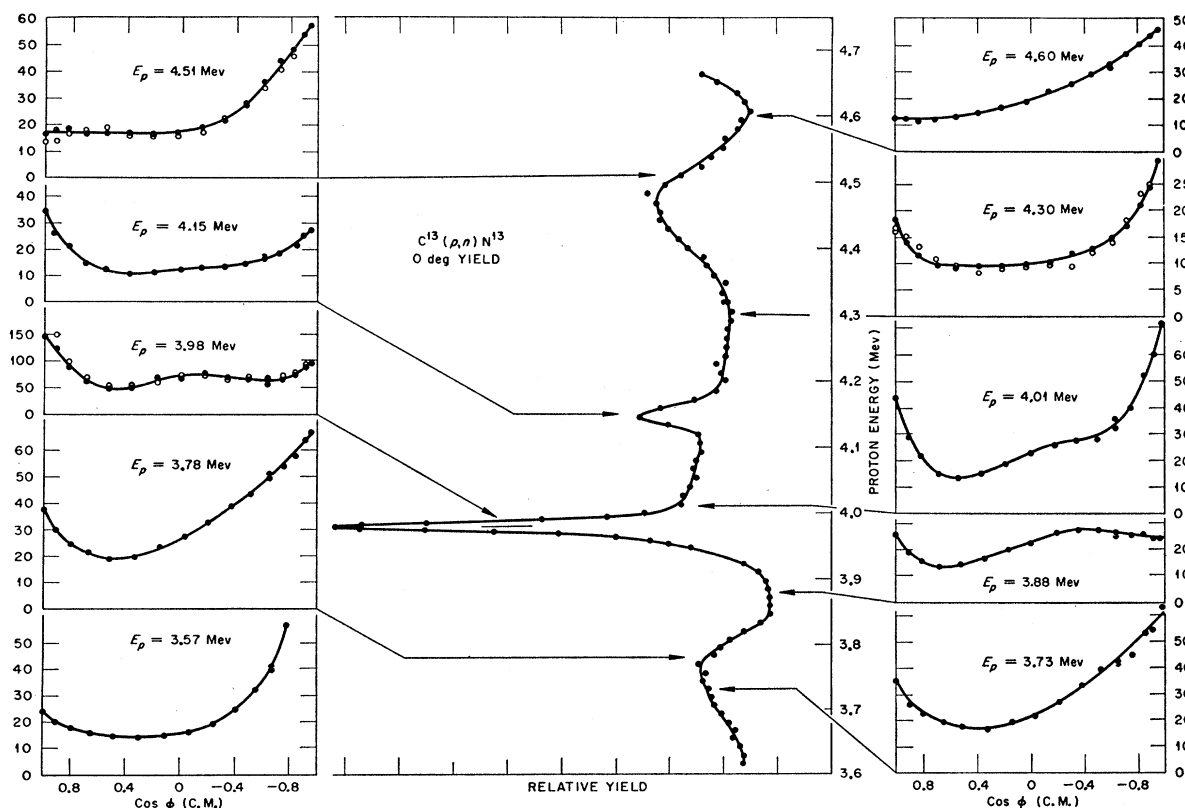


FIG. 4. Plotted in the center with proton energy running vertically is a section of the $C^{13}(p,n)N^{13}$ 0° yield curve. The inserts are the angular distributions taken at the proton energies indicated by the arrows.

with a suitably biased propane recoil counter. Figure 4 gives the 0° neutron yield. Table I lists these results for the levels involved.

Neutron angular distributions were taken at 10 proton energies between 3.5 and 4.6 Mev. These data were obtained by means of the 1-in. \times 4-in. propane ($\frac{1}{2}$ atmosphere) recoil counter at a distance of about 3 in. from the target to the front face of the counter. Figure 4 shows a curve of the yield of neutrons in the forward direction and the neutron angular distributions (as a function of the cosine of the center-of-mass angle ϕ). The arrows indicate the proton energy at which the distribution was measured. The open points on the distribution at 3.98-Mev were taken some years ago using the long counter as the detector. The open points on the distributions at 4.30 and 4.51 Mev were taken using the propane recoil counter, but in a somewhat different experimental arrangement. The agreement between the various data is reasonable.

V. DISCUSSION

Since the lower energy inelastic scattering gamma rays arise from the known 3.09 Mev, $J=\frac{1}{2}^+$ state in C^{13} , their angular distributions always should be isotropic and hence cannot assist in spin assignments to the levels of the compound nucleus. The fact that all observed angular distributions of the 3.09-Mev gamma ray are isotropic is, of course, a confirmation of the previously assigned $J=\frac{1}{2}$ spin for the 3.09-Mev level.

The 3.68-Mev gamma ray resonance at a proton energy of 4.52-Mev can be fit satisfactorily in the j - j

coupling scheme by assuming that the level is 1^+ with entrance $j=\frac{3}{2}$ and exit $j=\frac{1}{2}$. No fit could be obtained for L - S coupling under reasonable assumptions. For arbitrary channel spin mixtures a fit could be obtained for the following cases: (A) $J=1^+$ with 85 to 100% entrance $s=0$, with greater than 99% exit $s'=2$ and α positive, (where α is the ratio of the amplitude of exit channel spin 2 to that for exit channel spin 1); (B) $J=1^+$ with 69 to 100% entrance $s=0$, with greater than 34% $s'=2$, with α negative; (C) $J=2^-$ with 8% entrance $s=0$, and 100% exit channel spin $s'=2$; (D) $J=2^+$ with all entrance $s=1$ and either 8% or 92% $s'=1$, α negative; and (E) $J=3^-$ with either 20% $s'=1$ or 93% $s'=1$, α negative. In the case of $J=2$, the $J=2^-$ is preferred by a penetrability argument which would also tend to reduce the excitation of the 3.09-Mev state in agreement with our low yield of the 3.09-Mev gamma ray. An unambiguous spin assignment cannot be made from these data.

No analysis of the neutron angular distributions has been attempted. The new values of the resonant energies bring our data into agreement with those of Gibbons and Macklin.⁵ Table I lists, in columns 5 and 6, the new energies for these 0° yield maxima and their differences from the old values. These new values are, as expected, lower than the old energies and the differences are of about the expected amount. Column 7 gives the energy of the maxima of neutron yield in the backward direction. Column 8 gives an estimate of the experimental width (full width at half height).

⁵ J. H. Gibbons and R. L. Macklin, Phys. Rev. **114**, 571 (1959).